CFD MODELLING OF CONVECTIVE HEAT TRANSFER FROM A WINDOW WITH ADJACENT VENETIAN BLINDS

Ljiljana Marjanovic[1,2], Malcom Cook[2], Vic Hanby[2] and Simon Rees[2]
[1]Factuly of Mechanical Engineering, Belgrade University, Belgrade, Serbia and Montenegro
[2]Instititute of Energy and Sustainable Development, DeMontfort University, UK

ABSTRACT

This paper studies in three-dimension the coupled convective and radiative heat transfer rate from a window surface with adjacent aluminium venetian blind using commercially available CFD software. The flow patterns (temperature and velocity fields) and convective heat transfer coefficient were investigated for different blade angles (0^0, 45^0, -45^0, 80^0) for both summer and winter conditions. Comparisons were made with available experimental and other theoretical research.

The results of this paper indicate that heat transfer between window and indoor air is influenced significantly by the presence of an aluminium venetian blind and that the cellular flow between the blind slats can have an important effect on heat transfer from a window surface can only be fully recognized and analyzed in three dimensions.

INTRODUCTION

The window, due to its potentially large heat gains in summer and losses in winter, has been the subject of much research. The thermal performance of glazing systems was first studied using the simple one-dimensional heat transfer analysis, (Ye 1999, Curcuja 1993). Two dimensional flow modeling has shown that one dimensional heat transfer may lead to invalid results where two and three-dimensional effects are present, (Curcija 1993). Experimental studies using Mach-Zehnder interferometer to measure local convection coefficients on the plate for several slat angles and blind-to-window spacings showed that venetian blinds cause a strong periodical variation in local convection coefficient for certain angles, especially when the blinds are placed close to window, (Machin 1998). Recently several two dimensional finite element studies of this problem have been reported (Ye 1999, Philips 2001). Radiation hasn't been taken into account in (Ye 1999) and in earlier work by Philips and Naylor, (Philips 1999). Both papers concluded that when the blinds are placed closely to a window surface (less than 20mm) radiation is a significant factor and should be taken into account. Later two dimensional studies did take radiation into account. However, there is limited three-dimensional information on the performance of glazing systems with blinds.

In this study a three-dimensional numerical solution has been obtained on the effect of a venetian blind on the conjugate heat transfer from an indoor window glazing. A solution has been obtained for the coupled laminar free convection and radiation heat transfer problem including conduction along the blind slats.

THE MODEL AND ITS PARAMETERS

The continuity, momentum and energy equations for buoyant flow assuming steady, laminar and incompressible flow were solved using commercially available CFD software. Grey diffuse radiation exchange between the window, blind and air has been considered using the Monte Carlo Method. All thermophysical properties of air were assumed to be constant except for density which was modelling with the Bousinesq approximation. Both winter and summer conditions were taken into account. For summer conditions so cold night case where no incident solar radiation is present was investigated.

The window surface is fixed at a temperature T_w and the ambient at T_∞. In the computational domain the window represents an isothermal type boundary condition with no slip (zero velocity). The height of the domain has been extended beyond the blinds to allow for inflow and outflow regions. Fluid is allowed to entrain into the computational domain at ambient temperature in a direction perpendicular to the window. On the far left and far right end of the venetian blinds, zero derivate boundary conditions were applied. At the blind slat surfaces the boundary condition was set up as an adiabatic wall.

Computational domain and boundary conditions are presented in Figure 1. The geometry of the model approximates real model. In practice windows would have frame effects and only the center-of-the glass region would be nearly isothermal. However the idealized geometry allows comparison with published data since it is a common assumption in both theoretical and experimental consideration of this problem. The assumption that the flow is laminar was made in both (Ye 1999) and (Philips 2001). The values obtained for Reynolds numbers in this work in general support that assumption as it will be discussed later in the paper.

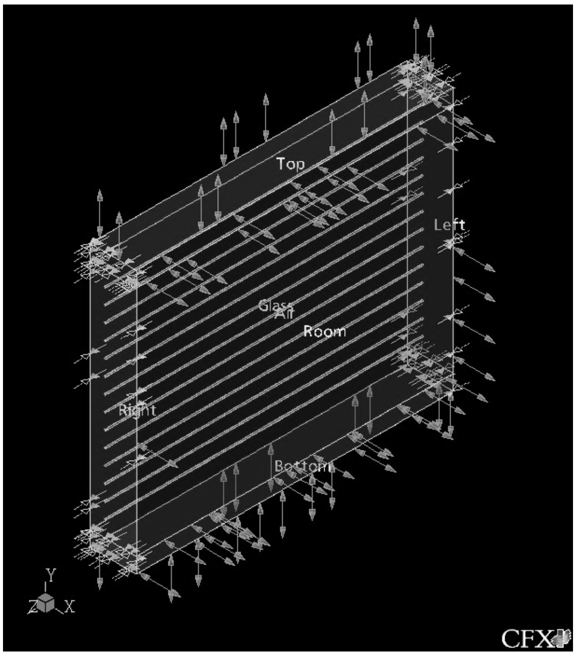

Figure 1 Computational domain

The venetian blind is placed at a distance *b* from the window and each blind slat is set at angle θ from the horizontal. The slats have width of 25.4mm and thickness of 3mm which are typical dimensions for commercially available blinds. The blind slats have conductivity k_B and emissivity ε_B and exchange thermal radiation with the window with emissivity ε_W and the air with emissivity ε_∞. The overview of the model parameters is presented in Table 1.

Table1
Model parameters

Window height L [mm]	430
Window width [mm]	57
Window emissivity ε_W [-]	0.84
Blind width [mm]	25.4
Blind thickness t [mm]	3
Blind emissivity ε_B [-]	0.8
Blind (Al) conductivity k_B [W/mK]	115
Blind/win distance b [mm]	15
t_w/t_∞ [^{0}C] for summer conditions	43/21
t_w/t_∞ [^{0}C] for winter conditions	5/21

Aluminum blinds of emissivity 0.8 and conductivity of 115 W/mK were chosen according to (Philips 2001) as a first published numerical study of the problem to include radiation. The emissivity of 0.84 represents a typical value for window glass. In this paper the emphasis is placed on results for venetian blind distance from a window of 15mm since at smallest distances the blind has the strongest interaction with heat transfer from a window. This distance is also very common in practice. The temperature difference between the window and the room for summer conditions is 22K which is the same value assumed in (Ye 1999) and very similar to Machini's experiments (Machin 1998). Philipas at al (Philips 1998) have chosen temperature difference around 10K and thus lower temperature values for the window surface.

Due to a very complicated geometry and combined air flow, heat transfer and radiation modelling, a very fine grid had to be formed. For the blind angle of 0^0 the total number of grid elements in fluid domain was over 1.3 millions of which 29469 were used in radiation modeling and the total number in solid domain (blinds) was 81708 coursen to 2673 for radiation modeling. For partially closed blinds (blind angles of +/-45^0) the number of grid elements had to be increased almost 3 times for fluid domain leading to over 3.7 millions for air domain and 93400 for solid domain with similar coarsening rates. In all cases grid numerical independence has been achieved.

VALIDATION OF THE MODEL

The CFD code used in this research was fully validated for the case of vertical isothermal plate, (Zitzman 2005). Since the theoretical solution for a vertical plate with adjacent venetian blinds does not exist, a qualitative comparison with experimental results in (Machin 1998) and numerical solution presented in (Philips 2001) for summer conditions was performed. Both temperature and velocity fields were compared. Since the flow visualization experiment in (Machine 1998) did not result in stable picture for the slat angle of 45^0 but the smoke visualization image was changing constantly, the recommendation that only the results for slat angles of 0^0 and –45^0 should be used for validation purposes has been followed in this paper.

The numerical solution against which the validation has been performed is a 2D simulation. Since the simulation presented in this work is a 3D simulation, the 2D results were compared with a 3D results presented in a central vertical plate. Figure 2 shows the temperature contours obtained in (Philips 2001) and the contours in the central vertical plate from 3D simulation in this research. In each case the model parameters were the same, except the window temperature. Rayleigh numbers calculated in respect to window height L and given by equation 1 were thus of the same order of magnitude, $5x10^7$ and $1x10^7$ for this research and in (Philips 1998) respectively.

$$Ra_L = \frac{g\beta(T_w - T_\infty)L^3}{\alpha\nu} \qquad [1]$$

Strong similarity between the obtained numerical solutions for the temperature fields is obvious.

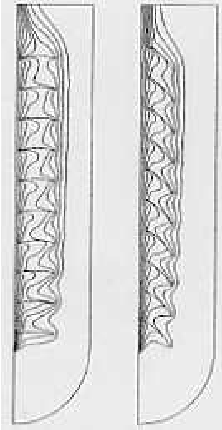

Figure 2a 2D simulation results for slat angles of 0^0 and -45^0 obtained in (Philips 2001)

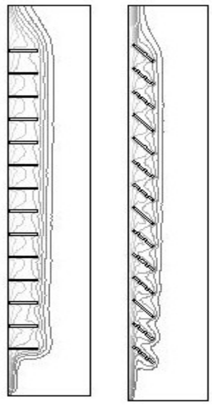

Figure 2b Current simulation results

Figure 2 Temperature contours comparison for different slat angles

Figure 3 shows the comparison between experimental flow visualization (Machin 1998) and numerical results (Philips 2001) with the streamline functions in central vertical plate of the domain shown in Figure 1.

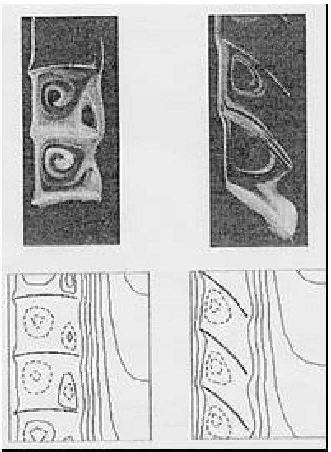

Figure 3a Flow visualization, (Machin 1998), and stream lines, (Philips 2001)

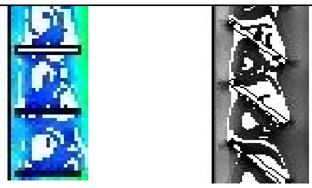

Figure 3b Current simulation results

Figure 3 Stream functions comparison for different slat angles

Machin in his experiment used somewhat different emission characteristic of materials leading in emissivity of 0.1 for window surface and 0.75 for venetian blinds. Temperature difference between hot plate (window) and bulk air is about 20K what is very similar to 22K used in this research. Rayleigh number in experiment reported in (Machine 1998) was 1.7×10^7. The simulation results in Figure 3 are confirming the existence of the dominant eddies for both 0^0 and -45^0 slat angels.

RESULTS AND DISCUSSION

Summer conditions

The influence of the slat angle on the flow was investigated comparing the heat transfer coefficients and the air flow fields for four different slat angles $\theta=0^0$, $+45^0$, -45^0 and 80^0. Convection heat transfer coefficient from the window plate for different slat angles is given in Figures 4. While air fields appear to be mainly uniform for open blinds (slat angle of 0^0) and slat angels of -45^0 and 80^0, for slat angle of 45^0 clear 3D air flow dependence can be observed.

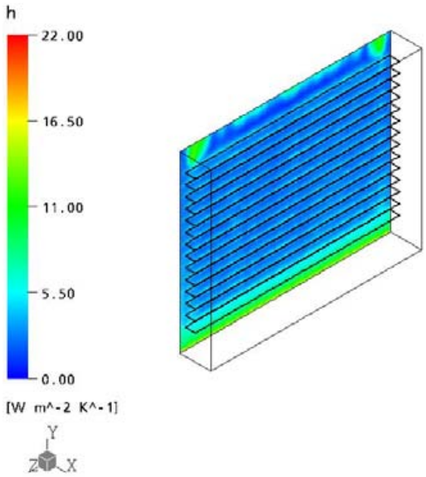

Figure 4a Wall heat transfer coefficients for open blinds for summer conditions

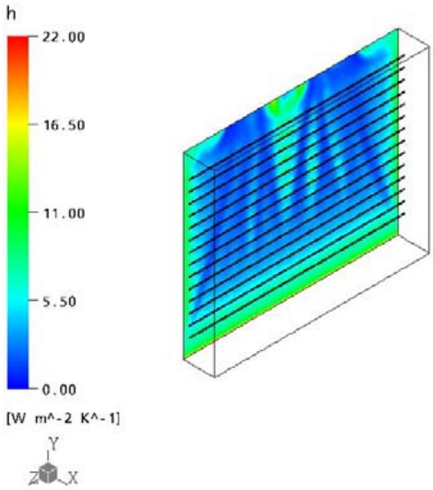

Figure4 b Wall heat transfer coefficients for partially closed (45^0) blinds for summer conditions

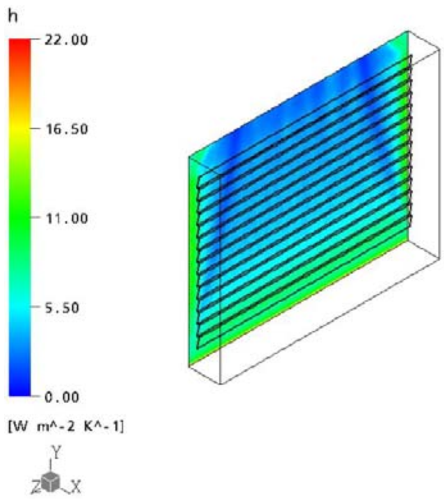

Figure 4c Wall heat transfer coefficients for closed blinds for summer conditions

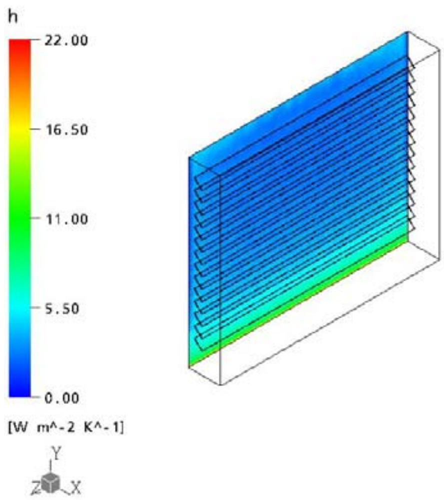

Figure 4d Wall heat transfer coefficients for partially closed (-45^0) blinds for summer conditions

Temperature contours for different slat angels in the central vertical plate are given in Figure 5, while velocity vectors are given in Figure 6.

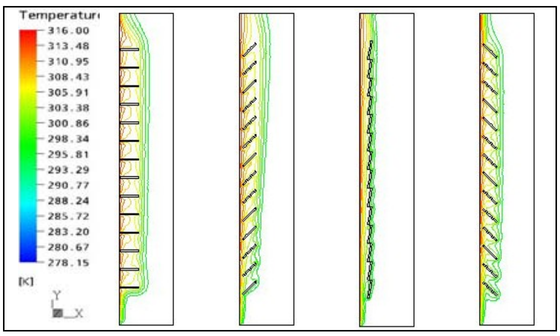

Figure 5 Temperature contours for different slat angels for summer conditions

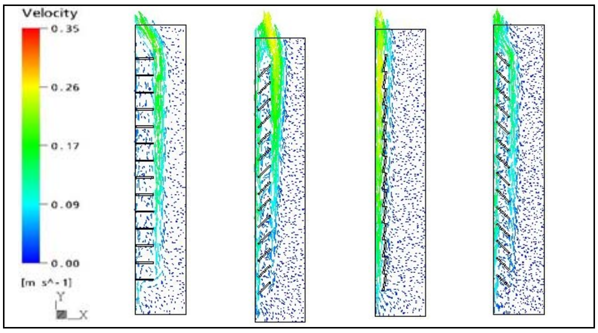

Figure 6 Velocity vectors for different slat angels for summer conditions

Local convection heat transfer coefficient along the central window surface for different slat angles is given in Figure 7 while average values for different blind angels are given in Table 2.

Table 2
Average convection heat transfer coefficients for summer conditions

	0^0	45^0	90^0	-45^0
h [W/m^{2}K]	3.96	4.42	5.31	3.74

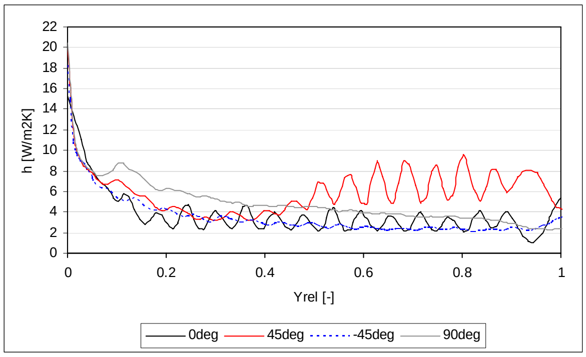

Figure 7 Local convection heat transfer coefficients for summer conditions

Winter conditions

Convection heat transfer coefficient from the window plate for different slat angles and winter conditions is given in Figures 8. Whilst for summer conditions a 3D air flow dependence was observed for slat angle of 45^0, this time clear 3D air flow dependence can be observed for -45^0 slat angle.

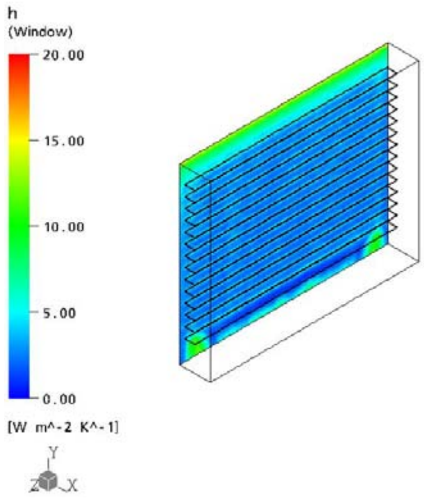

Figure 8a Wall heat transfer coefficients for open blinds for winter conditions

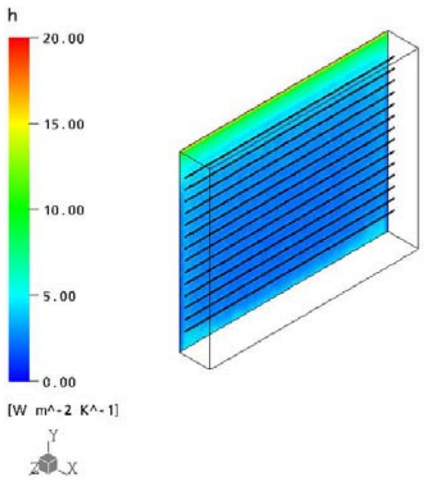

Figure 8b Wall heat transfer coefficients for partially closed (45^0) blinds for winter conditions

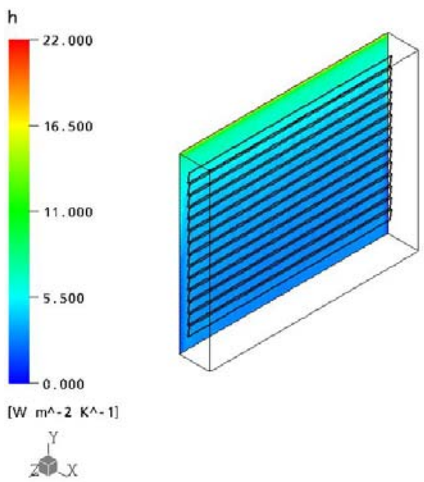

Figure 8c Wall heat transfer coefficients for closed blinds for winter conditions

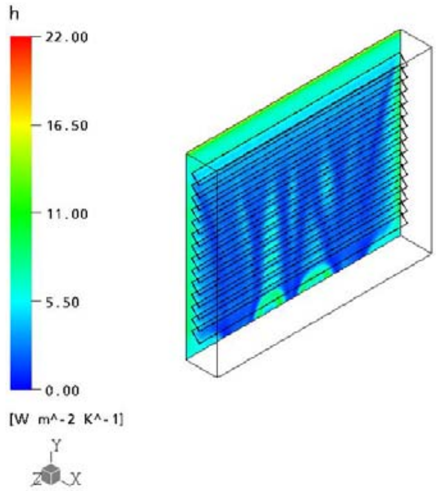

Figure 8d Wall heat transfer coefficients for partially closed (-45^0) for winter conditions

Temperature contours for different slat angels in the central vertical plate are given in Figure 9, while velocity vectors are given in Figure 10.

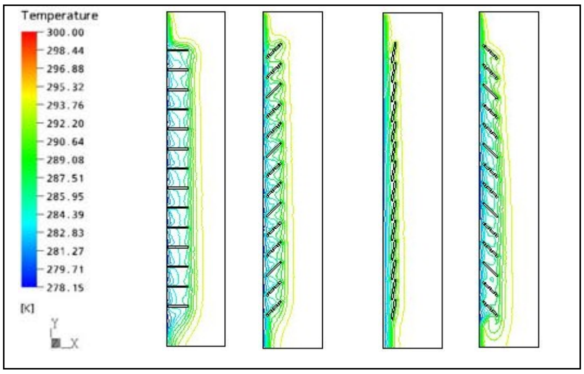

Figure 9 Temperature contours for different slat angels for winter conditions

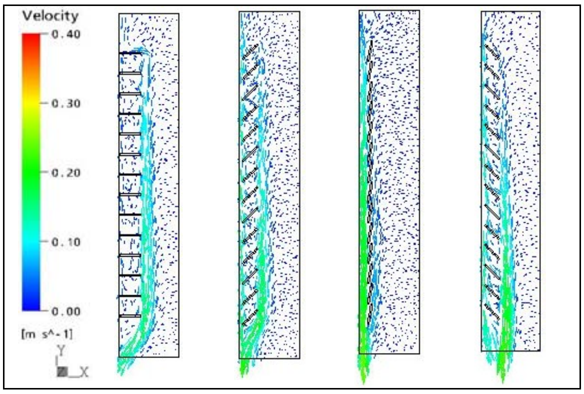

Figure 10 Velocity vectors for different slat angels for winter conditions

Local convection heat transfer coefficient along the central window surface for different slat angles is given in Figure 11 while average values for different blind angels are given in Table 3.

Table 3
Average convection heat transfer coefficients for summer conditions

	0^0	45^0	90^0	-45^0
h [W/m^{2}K]	3.74	3.43	4.28	3.89

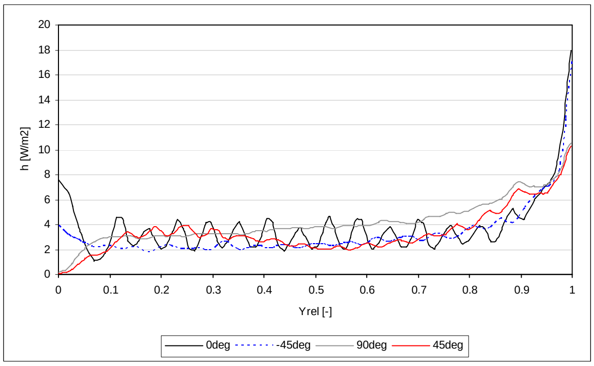

Figure 11 Local convection heat transfer coefficients for winter conditions

Results analysis

The presence of blinds introduces the disturbances in the flow field. Generally speaking three main areas of air motion can be observed regardless of blinds slat angle: the area between the glass surface and blinds, in between slats and in front of the blinds. The interaction of the blind with the free convection flow produces a spatial variation in convection heat transfer coefficient with frequency equal to the slat pitch. The disturbance decreases as the blind closes. However a symmetrical slat orientation of +/- 45^0 does not have a symmetrical effect as it can be observed for both summer and winter conditions (see Figures 4 and 8 respectively).

There are two major heat transfer mechanisms involved in this problem: conduction and convection. Conduction dominates when the fluid motion close to the window and between the slats is very week. Also slats can act as extended surfaces thus enhancing conduction heat transport. On the other hand when Rayliegh numbers are high enough, buoyancy driven eddies starts developing between the slats and the heat transfer becomes dominated by convection.

For both summer and winter conditions when the blinds are open the largest portion of air movement occurs in front of the blinds whilst very little air movements exists in the area between the glass surface and the blinds, see Figures 6 and 10. As the blinds close, the amount of air penetrating the area between the glass and the blinds increases. During this transition a more pronounced flow starts developing between the slats. However the amount of air and its velocity it's not the same for $+45^0$ slat orientation and -45^0.

Comparing the velocity fields for $\theta=45^0$ and $\theta=-45^0$, because the flow resistance for summer conditions is lower for the former case, velocities are higher and strong vortices are formed between slats preventing the cooler air flowing into the main stream near the hot window. This results in a lower temperature gradient near the window and therefore the lower heat transfer coefficient. For winter conditions compared to summer conditions the flow resistance is lower for the opposite slat angle and the vortices are formed between slats for -45^0.

An increase in magnitude in a periodic variation of heat transfer coefficient for summer conditions can be observed in Figure 7 for slat angle of 45^0 and for winter conditions in Figure 11 for slat angle of -45^0. However since for winter conditions the Rayliegh number was lower compared to summer conditions ($3.8\cdot10^7$ compared to $5.7\cdot10^7$), the overall value of heat transfer coefficient and its increase is smaller in winter compared to summer, see Figures 4b and 8e and Figures 7 and 11.

Oscillatory patterns of convection heat transfer coefficient are characteristically for the case of multicellular flow in cavities, (Gustavsen 2001, Zhai 1997). Increases in the periodic variation amplitude of convection heat transfer for certain geometries when the blinds are placed close to a window surface could imply the existence of a secondary flow. The appearance of the secondary flow in double glazed windows have been investigated in (Gustavsen 2001) and (Zhai 1997). When secondary flow appears, temperature profile starts oscillating and thus local Nusselt number or convection heat transfer coefficient, (Gustavsen 2001, Zhai 1997). When blinds are very close to a window surface, the blind-glass forms a cavity like region and the air motion may be governed and influenced by the same mechanisms as in the case of sealed cavity.

Increase in the amplitude of heat transfer coefficient typical for the case of secondary flow are clearly observed in Figure 7 only for $\theta=45^0$ and in Figure 11 for only $\theta=-45^0$. Existence of the multicellular flow increases the convective heat transfer rate by introducing localized convective motion. Results presented in Figures 7 and 11 are showing that highest values for heat transfer coefficient are for the slat angels of 45^0 and -45^0 respectively.

For similar temperature differences (ΔT=20K) and lower Rayleigh no ($2.4*10^4$) it has been shown in (Zahi 1997) that 2D simulations fail to predict the secondary flow. If the results for summer conditions were to be analyzed and presented only in 2D form, the temperature and velocities might be very different depending on the selected 2D plane as shown in Figure 12. The differences caused by 2D plane position for winter conditions is presented in Figure 13.

The likelihood of the secondary flow increases with the increase in Rayeligh number, (Gustavsen 2001, Zhai 1997). After a certain point further increase in Rayleigh number would result in the secondary flow disappearing, but the beginning of fully developed turbulent behavior. For the geometries where a clear 3D pattern has been observed (slat angle of $+45^0$ for summer conditions and -45^0 for winter conditions) Reynold numbers were only just above 10^3 while for all other cases were bellow critical value thus suggesting that in these two cases air flows were transitional. The intersection of stream lines which is characteristic for turbulent flow can be observed in Figures 12b and 13b.

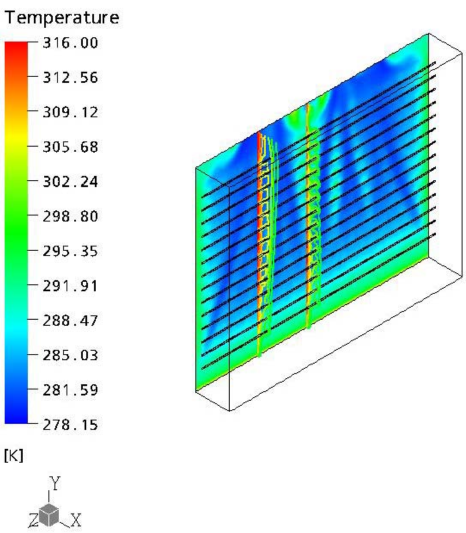

Figure 12a Convective heat transfer coefficient and temperature fields for different D sections

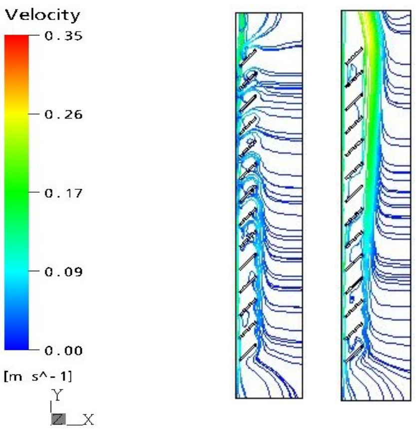

Figure 12b Stream lines in 2D sections in Figure12a

Figure 12 Dependence of 2D temperature and velocity fields on its position in 3D domain for summer conditions

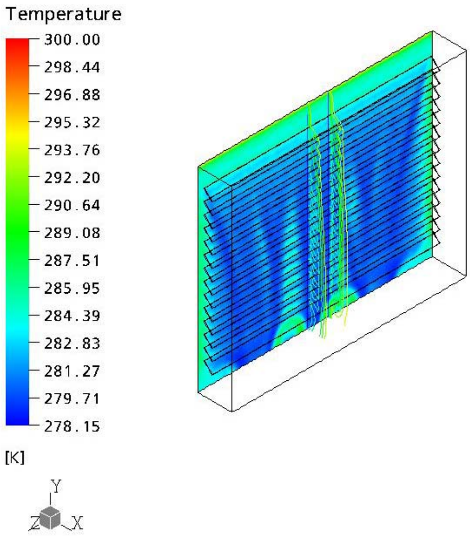

Figure 13a Convective heat transfer coefficient and temperature fields for different D sections for winter conditions

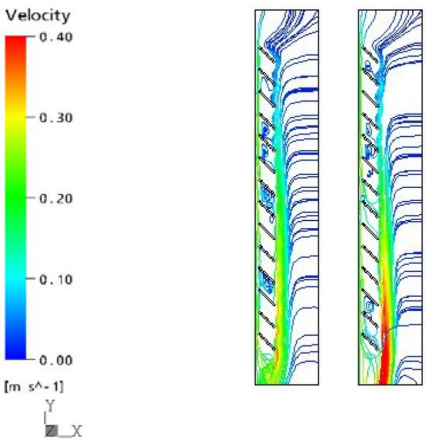

Figure 13b Stream lines in 2D sections in Figure13a

Figure 13 Dependence of 2D temperature and velocity fields on its position in 3D domain for winter conditions

CONCLUSIONS

The flow pattern (temperature and velocity fields) and convective heat transfer coefficient from the glazing surface were investigated for different blind slat angles (0^0, 45^0, -45^0, 80^0) for both winter and summer conditions.

The results of this paper show that heat transfer between window and indoor air is influenced both quantitatively and qualitatively by the presence of an aluminium venetian blind and that the cellular flow between the blinds slats can have a significant effect on the convective heat transfer from the window surface that can only be fully recognized and analyzed in three dimensions.

NOMENCLATURE

g [m/s2] gravitational constant
β [1/K] volumetric expansion coefficient
T_w [K] window temperature
T_∞ [K] ambient temperature
L [m] window height
ν [m^2/s] kinematic viscosity
ά [m^2/s] thermal diffusivity

REFERENCES

Philips, J., Naylor, D., Oosthuizen, P.H., Harrison, S.J. 2001. Numerical Study of Convective and Radiative Heat Transfer from a Window Glazing with a Venetian Blind, *HVAC&R Research*, Vol7, no4, pp 282-402, ASHRAE

Ye, P., Harrison, S.J. , Oosthuzien, P.H. 1999. Convective Heat Transfer from a Window with a Venetian Blinds: Detail Modeling, *ASHRAE Transaction*, pp 1031-1037, ASHRAE

Philips, J., Naylor, D., Harrison, S.J., Oosthuizen, P.H. 2001. Free Convection from a Window Glazing with a Venetian Blind: Numerical Model Development, *Transactions of CSME*, vol 23, no1B, pp159-172, CSME

Machin, A.D., Naylor, D., Harrison, P S.J. , Oosthuizen, H. 1998. Experimental Study of Free Convection at an Indoor Glazing Surface with a Venetian Blind, *HVAC&R Research*, Vol 4, no 2, pp 153- 166, ASHRAE

Curcija, D., Gross, W.P. 1993. Two dimensional natural convection over the isothermal indoor fenestration surface – Finite element numerical solution, *ASHRAE Transaction*, pp 274-287, ASHRAE

Gustavsen, A., Griffith B.T., Arasteh, D. 2001. Natural Convection Effects in Three-Dimensional Window Frames with Internal Cavities, ASHRAE Transactions, Vol 107 (2), ASHRE

Zahi, Y., Curcija, D., Godd, W. 1997. Prediction of the Multicellular Flow Regime of Natural Convection in Fenestration Glazing Cavities, ASHRAE Transactions, Vol 103 (1), pp. 1009-1020, ASHRAE

Zitzmann, T., Cook, M., Rees, S.J., Pfromer, P., Marjanovic, Lj. 2005: Modelling free convection and heat transfer in a room with CFD and validation (accepted for BS 2005)